ISSN: 0067-2904

Kinetics of Struvite Crystals Formation through Adsorption and Crystallization Using Zeolite Modification

Eko Ariyanto[1]*, Dian Kharismadewi [1], Mardwita Mardwita [1], Stefanus Muryanto[2]
[1]*Departement of Chemical Engineering, Engineering Faculty, Universitas Muhammadiyah Palembang, Palembang, Indonesia*
[2]*Department of Chemical Engineering, UNTAG University, Semarang, Indonesia*

Received: 11/6/2022 Accepted: 1/1/2023 Published: 30/1/2024

Abstract

This study observed the formation of struvite crystals in wastewater using natural zeolite activated with Mg^{2+} ions. Mg^{2+} ions released from natural zeolite would react with PO_4^{3-} and NH_4^+ ions from in wastewater to form struvite crystals. The results showed that at pH 8.5, the removal of PO_4^{3-} and NH_4^+ ions was more effective using the modified zeolite than the natural zeolite. Adding 40 g/L Zeo-Mg (1) produced the best results, with $PO4^{3-}$ (93.32%) and NH_4 (40%) adsorption. Meanwhile, 40g/L Zeo-Mg (2) adsorbed 81% PO_4^{3-} ions and 27.12% NH_4^+ ions. The eqilibrium time of all the treatments was 40 min. The results of observation through SEM, EDX, and FTIR showed that struvite crystals were formed on the zeolite surface. Kinetic models indicated that the mechanism of struvite formation on the surface of natural and modified zeolite was mainly chemisorption. Further calculations showed that the adsorption of PO_4^{3-} and NH_4^+ ion followed the pseudo-first-order kinetic model.

Keywords: Struvite, Natural Zeolite, Crystallization, Equilibrium Studies

1. Introduction

Because of the anaerobic digestion of organic waste in the wastewater treatment plant, magnesium (Mg^{2+}), ammonium (NH_4^+), and phosphate (PO_4^{3-}) ions are released. These ions can react to produce struvite crystals under specific conditions, such as pH 8.0-9.5 and ion concentrations that exceed those of the supersaturated solution [1-5]. Many chemical compounds, such as solid or liquid organic pollutants, inorganic fertilizer, heavy metals, or hazardous materials, have entered wastewater due to industrial or human activities. Over time, those compounds may precipitate to form solid material and eventually degrade in a wastewater treatment plant. However, under specific physicochemical conditions, the dissolved Mg^{2+}, NH_4^+, and PO_4^{3-} ions in wastewater can react to form struvite, causing hard-scale pipe surfaces or pipe blockage that inhibits the flow process. Consequently, it increases pumping costs, reduces plant capacity [6,7], and further affects the working processes of centrifuges, heat exchangers, and aerators. The struvite crystal is formed under alkaline conditions based on reaction Eq. (1) [8,9] as follows:

$$Mg^{2+}(aq) + NH_4^+(aq) + PO_4^{3-}(aq) + 6H_2O \rightarrow MgNH_4PO_4 6H_2O \downarrow \quad (1)$$

* Email: eko_ariyanto@um-palembang.ac.id

Although struvite crystal formation has long been the main problem, struvite crystal is a potential slow-release fertilizer, so wastewater treatment companies attempt to recover the wastewater by removing PO_4^{3-} and NH_4^+ ions [9]. According to Mijangos *et al*. [10], PO_4^{3-} and NH_4^+ ion concentrations can be removed using natural zeolite activated with Mg^{2+} ions to form struvite crystals. The struvite crystals are formed through a two-step mechanism: ion exchange and struvite formation. In this mechanism, physical adsorption of NH^{4+} on the zeolite surface occurs in this mechanism, and then Mg^{2+} reacts with PO_4^{3-} and NH_4^+ ions to form struvite crystal, which adheres to the zeolite surface [10, 11]. It is essential to study the struvite formation in natural zeolite and modified zeolite, especially the adsorption mechanism. Previous studies reported that the benefits of removing the concentrations of NH_4^+ ions from solutions using zeolite include low cost, a simple process, and an easy procedure [12]. Zeolites are crystalline, microporous aluminosilicate minerals consisting of three-dimensional frameworks of SiO_4^{4-} and AlO_4^{5-} tetrahedral linked through shared oxygen atoms [13,14]. Zeolite with a low or intermediate ratio of Si/Al can be hydrophilic and act as a proper ion exchanger to remove heavy metals and radioactive compounds [15]. Zeolite is frequently employed as an ion exchanger in domestic and commercial water purification, softening, and other applications because of its high selectivity for ammonium and metallic ions [16,17]. Although natural zeolite can be easily applied in the adsorption process, it is necessary to improve the adsorption capacity [11] through treatments using acids, alkalis, and salts [18,19], calcination [20], microwave pre-treatment [21], and electrochemical treatment [22]. Research by Lin *et al*. [17] on natural zeolite modified with NaCl solution showed that NaCl-modified zeolite adsorbed more NH_4 than natural zeolite. Accordingly, despite the capacity to remove PO_4^{3-} and NH_4^+ ions simultaneously, the efficiency rate was relatively low [11,23]. Another method for the simultaneous removal of NH_4^+ ions is a combination of ion exchange and struvite formation. The rate of NH_4^+ ion adsorption on zeolite is strongly influenced by the pH of the solution because of the competing actions of H^+ and the fact that pH affects the ionization of the functional groups on the sorbent material's surface [24-26]. The optimum pH of 6-7 [27], 7 [24], and 8 [25,28], for removing NH_4^+ ions using zeolite has been reported. Previous studies mentioned above have suggested the following Equation (2) that mainly performs the removal of NH_4^+ ions by zeolite [28]:

$$\text{zeolite} - Mg^{2+} + NH_4^+ \leftrightarrow Mg^{2+} + \text{zeolite} - NH_4^+ \quad (2)$$

Equation 2 illustrates the mechanism of ion exchange between Mg^{2+} and NH_4^+ ions in zeolite. The Mg^{2+} ions released will react with the PO_4^{3-} and NH_4^+ ions in the solution. Mg^{2+} ions are crucial in the formation of struvite crystals in zeolite because the more Mg^{2+} ions are present in zeolite, the more sources of magnesium it must form struvite crystals [11]. Furthermore, Equation 2 shows that struvite crystals can be formed in solutions with pH greater than 7. The aim of this study is to determine the effect of pH, reaction time, and reagent dosage of the natural and modified zeolites on the removal of PO_4^{3-} and NH_4^+ ions. We also referred to batch adsorption studies on natural and modified zeolites to identify the reaction kinetics and mechanism of adsorption of PO_4^{3-} and NH_4^+ ions.

2. Materials and methods

2.1. Materials

2.1.1. Preparing zeolite modification

The zeolite used in this study was derived from CV. Minatama, Bandar Lampung, Lampung Province, Indonesia, with a Si/Al ratio of 4/1 (% w/w). The samples of natural zeolite were pulverized to a 100-mesh particle size. Impurities such as salinity, sand specimens, and ash from natural zeolite were removed by washing it with distilled water. Then, the clean natural

zeolite was dried at 100 ± 1 °C for 12 hours. The natural zeolite was modified at two temperatures: at 80 °C, named Zeo-Mg (1), and at room temperature, named Zeo-Mg (2). The preparation of zeolite Zeo-Mg(1) followed the research method described by Saputra *et al*. [29]. One hundred grams of pulverized natural zeolite were placed into $MgCl_2$ solutions (1 L of 2 mol/L). The mixture was heated to 80 °C and stirred for 6 hours in a refluxing flask, after which the zeolite was filtered. The mixture was mixed three times for maximum ion exchange before being oven-dried at 100 °C for 12 hours. In the preparation of Zeo-Mg (2), after the dispersion of natural zeolite was complete, the mixture was left to stir for 6 hours at room temperature and repeated three times.

2.1.2. Solution preparation

The synthetic wastewater solution was prepared by dissolving analytical-grade $KHPO_4$ and NH_4Cl into distilled water as sources of PO_4^{3-} and NH_4^+ ions, respectively. The concentration was simulated with PO_4^{3-} and NH_4^+ ion concentrations of 5 and 35 mM, respectively.

2.2. Experimental methods

Natural and modified zeolites of Zeo-Mg (1) and Zeo-Mg (2) were used in experiments to examine the PO_4^{3-} and NH_4^+ ions removal from solutions at various pH levels and adsorbent dosages. The experiments were subsequently performed to achieve optimum conditions and identify the pH, adsorbent dosage, and equilibrium at which time the optimum conditions occur. PO_4^{3-} and NH_4^+ ion solutions were mixed in a beaker glass at pH 7.8. In order to reach the desired pH, solutions were added with NaOH and HCl. The pH of the solution was determined using a digital pH meter and adjusted to the desired value using a stock solution of NaOH (0.05 M) and HCl (0.05 M). Pouring synthetic wastewater (500 mL) containing PO_4^{3-} and NH_4^+ ions into a 1,000 mL beaker while stirring at 100 rpm was used to conduct the experiment. Then a specific dose of adsorbent was added to the synthetic wastewater. Synthetic wastewater (2 mL) was taken at a specific time to analyze PO_4^{3-} and NH_4^+ ion removal using spectrophotometry (Hanna HI83300-02). The synthetic wastewater was filtered through a 0.2 µm filter membrane when the contact time was over. The adsorbent obtained was dried in an oven at 35 °C for 24 hours. The elemental morphology composition of the adsorbent was then examined using a scanning electron microscope with energy dispersive X-rays (SEM-EDX). The composition of the natural and modified zeolites was analyzed by FT-IR spectroscopy. A nitrogen gas adsorption analyzer determined the specific surface area, pore volume, and pore radius of natural and modified zeolites. The amount of adsorbate adsorbed at time t, and the percentage of removal of PO_4^{3-} and NH_4^+ ions into natural zeolite and modified zeolite were calculated using Equations 4 and 5, respectively [30].

$$Q_t = \frac{(C_o - C_t)V}{m} \quad (4)$$

$$\%\ \text{removal} = \frac{(C_o - C_t)}{C_o} \times 100 \quad (5)$$

where C_o is the initial adsorbate concentration (mg/L), C_t is the concentration of adsorbate at any time t, V is the volume of the adsorbate solution, and m is the mass of the adsorbent in (g).

3. Results and discussion

3.1. Characterization of the solid adsorbent

The morphology of natural and modified zeolites identified using Scanning Electron Microscope (SEM) is illustrated in Figure 1. Figure 1a shows the morphology of natural zeolites after the activation process using Mg^{2+} ions. Figure 1b shows that the Zeo-Mg (1) resulting from the modification of natural zeolite using Mg^{2+} ions at a temperature of 80 ^oC, and Figure 1c shows that the Zeo-Mg (2) resulting from the modification of natural zeolite using Mg^{2+} ions at room temperature. After modification, some changes occurred to the structure of zeolite.

Mg^{2+} ions covered the surface of zeolite, on which pores appeared. Figure 1b shows more pores than in Figure 1c, indicating that heat during the activation process helped boost the ion exchange between the chemical components of zeolite and the Mg^{2+} ions of the solution.

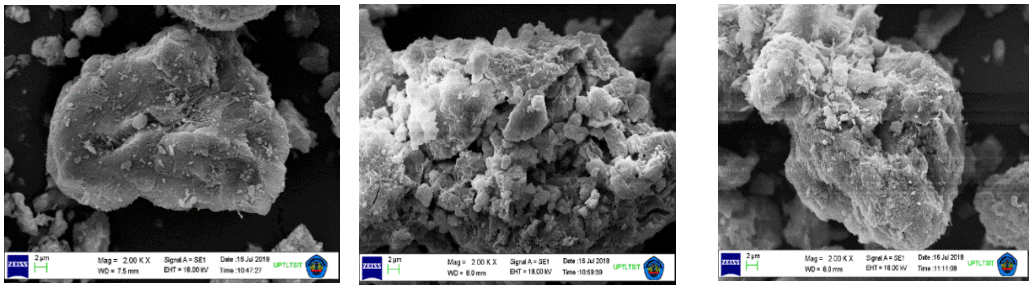

(a) (b) ©

Figure 1: SEM micrographs for natural zeolite: (a) before magnesium modification, (b) Zeo-Mg(1), and (c) Zeo-Mg(2)

The characteristics of natural zeolites, Zeo-Mg(1) and Zeo-Mg(2), were analyzed using an FT-IR analyzer in the range of 600-4000 cm^{-1} (Figure 2). Three peaks of adsorption bands were achieved at a significant rate after Mg^{2+} ion modification. The peak of the Mg-Zeo(1) adsorption band is higher than that of Mg-Zeo(2), which indicates that the temperature activated in Mg-Zeo(1) has successfully increased the number of Mg^{2+} ions at the surface of hydroxyl groups of in zeolite. According to Sadrara *et al*. [31]. The bonds between the 600 and 700 cm^{-1} regions are generally related to the specific fingerprint of secondary building units of framework structures in zeolites. The adsorption bands at 775 cm^{-1} confirmed the presence of the symmetric stretching of Si–C [32,56]. For natural zeolites, Zeo-Mg(1) and Zeo-Mg(2), Si-O-Si asymmetric stretching vibrations were observed at 1038, 1041, and 1045 cm^{-1}, respectively [33,34]. Figure 2 indicates that the adsorption bands at 3399, 3421, and 3455 cm^{-1} for natural zeolite, Zeo-Mg(1), and Zeo-Mg(2), respectively, were associated with the stretching bands of the hydrogen-bonded hydroxyl groups [35]. It was noticed that the absorbance of these peaks was increasing after the modification of zeolite with Mg^{2+} ions.

These results confirm the successful grafting of Mg^{2+} ions onto the surface hydroxyl groups of natural zeolite [32,56]. The stretching band at 3645-3600 cm^{-1} indicates a hydroxyl group within the solid sample layer [35]. According to Figure 2, the hydroxyl group of the experimental results is at 3622, 3623, and 3624 cm^{-1} for natural zeolites, Zeo-Mg(1) and Zeo-Mg(2), respectively.

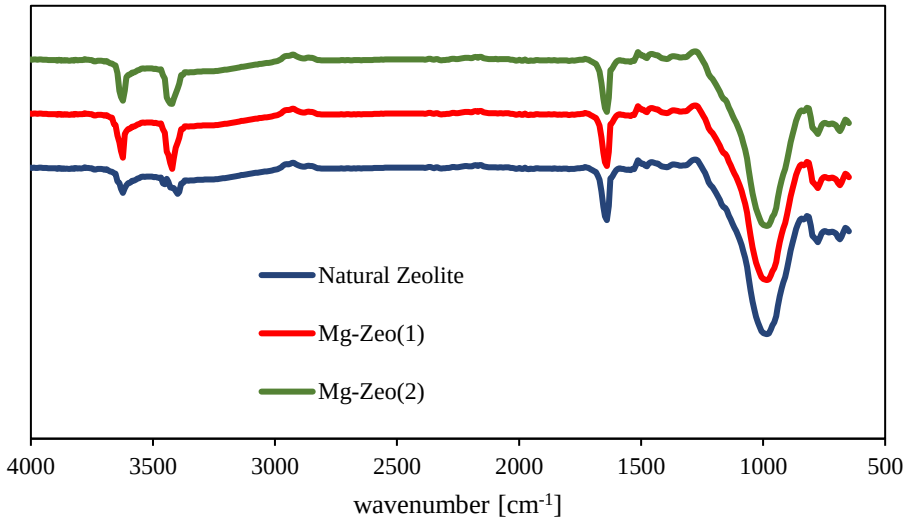

Figure 2: FT-IR spectra obtained for natural zeolite, Zeo-Mg(1) and Zeo-Mg(2)

The summarized BET analysis on surface area, pore volume, and pore radius of natural and modified zeolites can be seen in Table 1, which shows that the effect of zeolite modification can increase BET surface area, pore volume, and pore radius. The increase of surface area, pore volume, and pore radius is indicative of Mg^{2+} ion exchange from MgCl solution to K^{+}, Ca^{2+}, Fe^{+}, and Na^{+} ions in zeolite [36,55]. Table 2 shows an increase in surface area, pore volume, and pore radius from Zeo-Mg(1) compared to those in Zeo-Mg(2), which could be due to the release of K^{+}, Ca^{2+}, Fe^{+}, and Na^{+} ions as a result of heating when zeolite is modified with Mg^{2+} ions [37,38].

Table 1: The results of BET analysis

Types	BET surface area ($m^2.g^{-1}$)	Pore volume ($cm^3.g^{-1}$)	Pore radius (nm)
Natural Zeolite	31.05	0.064	26.16
Zeo-Mg(1)	38.26	0.096	35.45
Zeo-Mg(2)	34.32	0.071	30.54

Chemical element identification in natural zeolite and modified zeolite was identified using EDX. Table 2 shows an indication of a decrease in the content of K^{+}, Ca^{2+}, Fe^{+}, and Na^{+} ions after the natural zeolite modification process. On the other hand, Mg^{2+} ions increased on Zeo-Mg(1) and Zeo-Mg(2). It shows the occurrence of mass transfer in the zeolite modification process. At 80 °C, the mass transfer of Mg^{2+} ions on the Zeo-Mg(1) process was greater than at room temperature. This observation suggests that the K^{+}, Ca^{2+}, Fe^{+}, and Na^{+} in natural zeolite were replaced by Mg^{2+} ions, so the Mg^{2+} ions in natural zeolite increased [11].

Table 2: Chemical composition of natural zeolite and modified zeolite by EDX

Chemicals elements	Natural zeolite (wt.%)	Modified zeolite	
		Zeo-Mg(1), (wt.%)	Zeo-Mg(2), (wt.%)
O	33.87	35.13	35.83
Si	49.71	46.96	48.01
Al	8.16	8.47	7.79
Na	1.53	0.61	0.62
Mg	0.63	5.43	4.71
K	1.14	0.38	0.32
Ca	2.59	0.32	0.43
Fe	3.51	2.47	2.29

The precipitates that formed at the optimal reaction conditions were collected from the experiment, and the solid was then analyzed by SEM-EDX and FT-IR to confirm our studies. The SEM images (Figures 3a, 3b, and 3c) illustrate the presence of struvite on the surface of zeolite. The Mg, P, and O peaks (major elements in struvite) were seen in the EDX spectrum [2]. In Figure 4, FT-IR absorption spectra of struvite crystallized on natural zeolite and modified zeolite are shown. The first peaks were formed at 1006, 1002, and 1004 cm^{-1} for natural zeolite, Zeo-Mg(1), and Zeo-Mg(2), respectively. The second peak occurred at 1059, 1078, and 1088 for natural zeolite, Zeo-Mg(1), and Zeo-Mg(2), respectively. These peaks indicated the presence of phosphate ions [35]. The peak became weak and broad at 1617, 1625, and 1618 cm^{-1} for natural zeolite, Zeo-Mg(1), and Zeo-Mg(2), respectively, due to the H–N–H or H–O–H scissoring effect [39]. The peaks for natural zeolite, Zeo-Mg(1), and Zeo-Mg(2) that occurred at 1435, 1423, and 1424, respectively, can be attributed to the N-H bending vibrations [35].

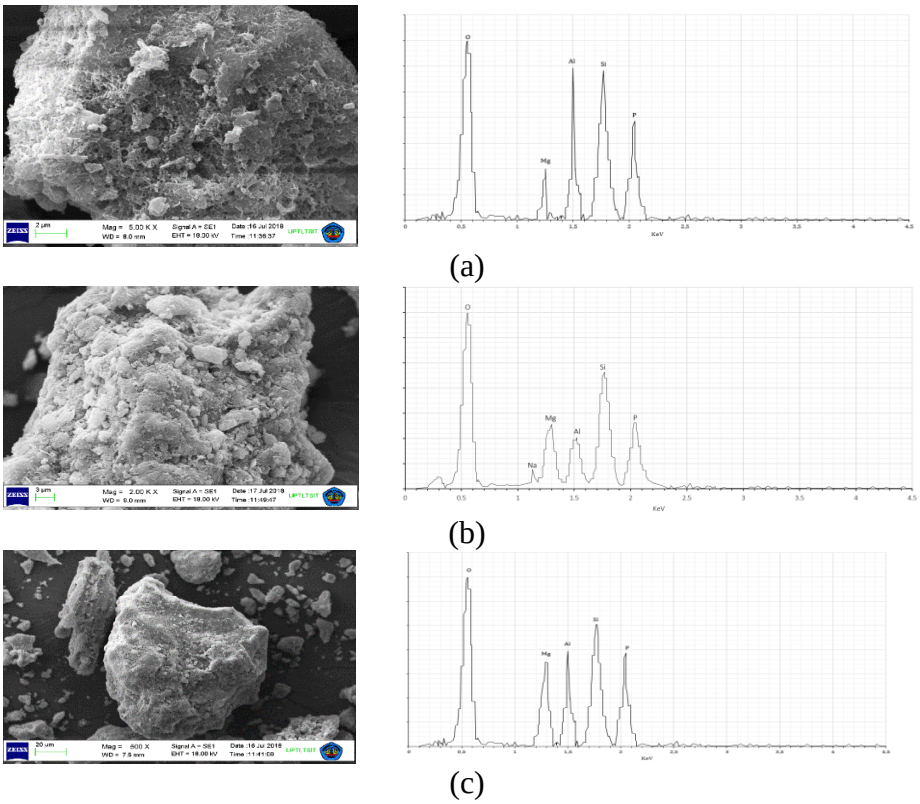

Figure 3: SEM image and EDX spectrogram of the solid from the precipitates collected using natural and modified zeolites

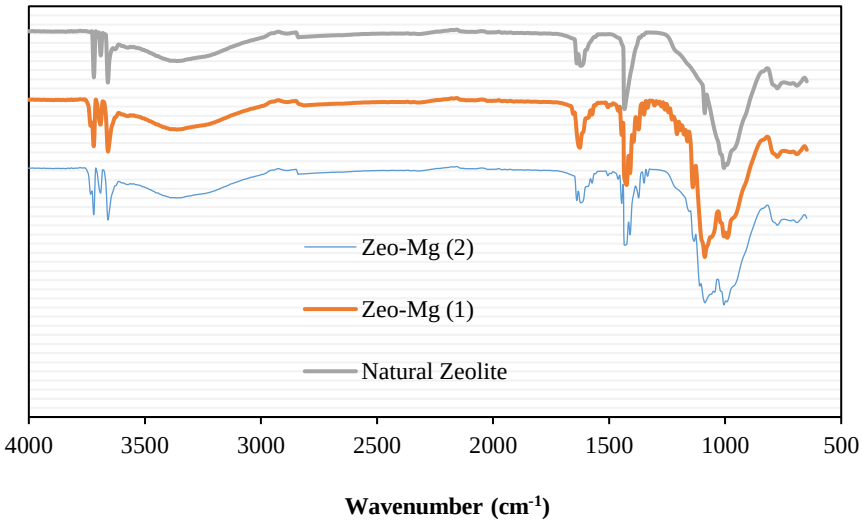

Figure 4: FT-IR spectrum of the struvite on Zeo-Mg(1), Zeo-Mg(2) and natural zeolite

3.2. Effect of pH on PO_4^{3-} and NH_4^+ ions removal

The pH of the solution is critical in the adsorption process of PO_4^{3-} and NH_4^+ ions on zeolites [40]. The adsorption of NH_4^+ ions on the surface of zeolite was influenced by the competitive effect of H^+ [24]. According to Chen *et al*. [41] and Hamdi and Srasra [42], increasing the pH of the solution in the range 4-9 decreases PO_4^{3-} ions adsorption on the zeolite. Adsorption of PO_4^{3-} ions was effective in an acidic pH range of 4-6 [42]. In this study, the removal of NH_4^+ and PO_4^{3-} ions was investigated at a pH range of 7-10 using natural and modified zeolites. The results are presented in Figures 5a and 5b. Figure 5a illustrates that more PO_4^{3-} ions were removed from the solution using modified zeolite, Zeo-Mg(1) and Zeo-Mg(2), between pH 7 and 8. The removal of PO_4^{3-} ions was greatest at pH 8.5 and decreased in the pH range of 9-10. The modified zeolite of Zeo-Mg(1) removed 92.32% of the PO_4^{3-} ions, which was higher than the removal of PO_4^{3-} ions by the modified zeolite of Zeo-Mg(2) and the natural zeolite. In other words, Zeo-Mg(1) modified zeolite increases the level of Mg_2^+ ions in zeolite, promoting the formation of struvite crystals on the zeolite surface. Furthermore, increasing the pH to 7-10 increased the removal of PO_4^{3-} ions. These findings may be attributed to the formation of amorphous calcium phosphate compounds [23]. Figure 5b shows that at a pH of 7-8, more NH_4 was removed from the solution using natural zeolites and modified zeolites - Zeo-Mg(1) and Zeo-Mg(2). The maximum level of removal occurred at pH 8.5, namely 42.45, 31.82, and 20.91% for modified zeolites Zeo-Mg(1), Zeo-Mg(2), and natural zeolites, respectively. Physical adsorption of NH_4^+ ions into the zeolite surface and electrostatic pull-in [43], which was attributed to ion exchange between Na_+ and Mg_2^+ ions, could be the cause. Mg_2^+ ions react with PO_4^{3-} and NH_4^+ ions to form struvite, which attaches to the surface of the zeolite. This study found that a high concentration of Mg^+ ions in Zeo-Mg(1) resulted in a decrease in high levels of PO_4^{3-} and NH_4^+ ions when compared to natural zeolite or Zeo-Mg(2). At pH > 8.5, less NH_4^+ was removed from solution, indicating that pH > 8.5 may have converted NH4 into NH3 gas, preventing zeolite from adsorbing NH_3 and resulting in less NH_4 removal [44,45]. From our findings, the optimum pH for the removal of PO_4^{3-} and NH_4^+ ions was 8.5 for all adsorbents. It indicates that struvite formed, Mg^{2+} ions just adsorbed on the surface of zeolite, Mg^{2+} ions entered the zeolite crystal lattice. Struvite crystallization results from the reaction of Mg^{2+}, PO_4^{3-}, and NH_4^+ ions. The reaction is significantly controlled over a pH range of 7-11. While struvite crystallization begins at pH 7.5 and peaks at pH 8.5 [46], Huang *et al*. [11] reported that struvite formation at pH 8-9.5 contributed to removing nutrients using modified zeolite. The removal of PO_4^{3-} and NH_4^+ ions by Zeo-Mg(1) modified zeolite at pH 8.5 was

92.39% and 42.45%, respectively. Compared to Huang *et al*. [11]. Compared to Huang *et al*. [11], this study used less zeolite (80g/L), but resulted in more removal of PO_4^{3-} and NH_4^+ ions.

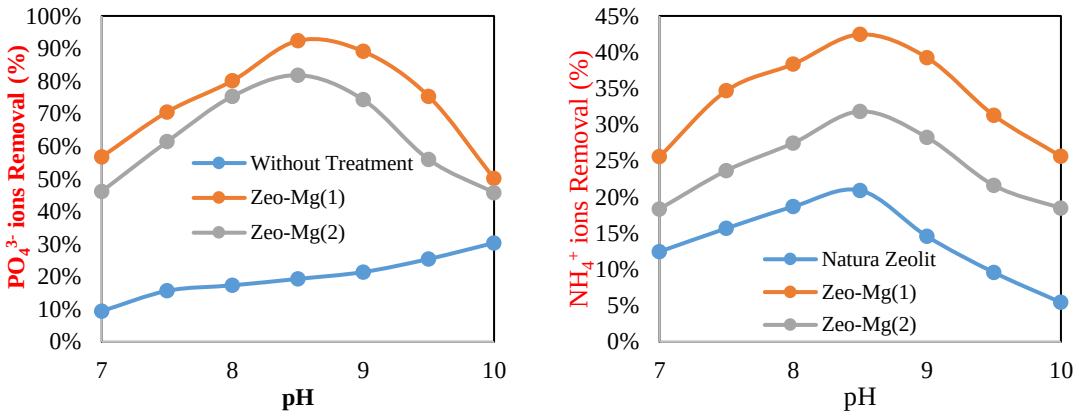

(a) (b)

Figure 5: Removal of PO_4^{3-} (a) and NH_4^+ (b) at different pH and modified zeolites (contact time: 40 minutes, adsorbent dosage: 80 g/L)

3.3. Effect of zeolite dosage on PO_4^{3-} and NH_4^+ ions removal

Figure 6 shows that the percentage of PO_4^{3-} and NH_4^+ ions removal increased with the dosage of adsorbent from 8 to 100 g/L for different types of zeolite modification. The removal rate of PO_4^{3-} and NH_4^+ ions is higher in Zeo-Mg(1) modification than in Zeo-Mg(2) and natural zeolite. For Zeo-Mg(1), removing PO_4^{3-} and NH_4^+ ions increased from 19.31 to 40.82 % and 50.00 to 92.90%, respectively, in the range of zeolite dosage. The equilibrium point was reached when more than 40 g/L adsorbent was added to modify Zeo-Mg(1) and Zeo-Mg(2), but a higher dosage would not affect the percentage of PO_4^{3-} and NH_4^+ ions removal.

This indicates that there are insufficient PO_4^{3-} and NH_4^+ ions ions in the solution to form struvite crystals. The equilibrium points of PO_4^{3-} and NH_4^+ ions removal occurred with the addition of 80 g/L natural zeolite. According to Huang *et al*. [11], increasing zeolite dosage tends to increase the magnesium concentration, while decreasing the ammonium concentration in the solution causes the decreased ammonium adsorption's driving force to be zeolite. According to Equation 1, the solution could be employed as a magnesium source for struvite crystallization by increasing the Mg^{2+} ion content. The results may also be responsible for forming aggregates at a higher solid-liquid ratio of particular precipitation [25]. Previous research, such as Huang *et al*. [11], which focused on the addition of Mg-zeolite modified with Mg2+ ions, found that the reaction of struvite crystals was capable of removing 90% of PO_4^{3-} and 81.2% of NH_4^+ ions when added with 110 g/L adsorbent at pH 8.5. Peng Xia *et al*. [47] investigated the effect of diatomite activation with MgO and found that when combined with 0.3 g/L adsorbent at pH 7, it removed 160,9 mg/g PO_4^{3-} and 77.05 mg/g NH_4^+ ions. In the current study, both PO_4^{3-} and NH_4^+ ions were efficiently removed when 40g/L of modified zeolite was added to the wastewater.

.

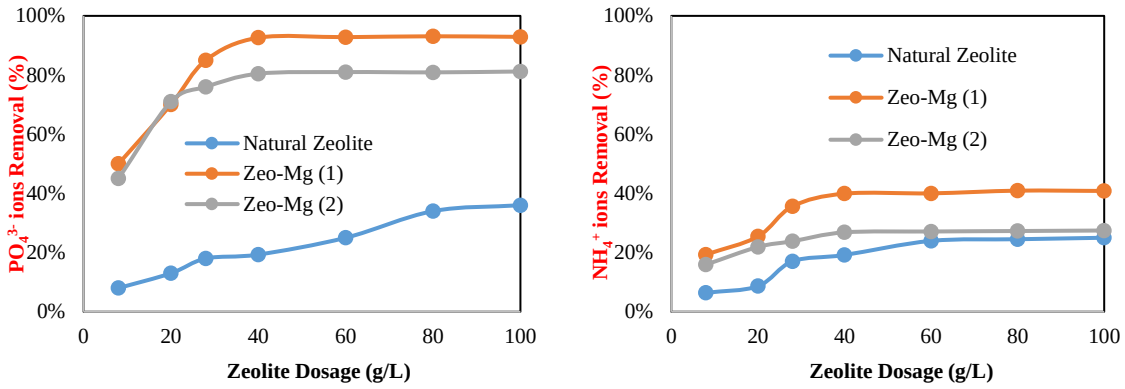

(a) (b)

Figure 6: Effect of zeolite dosage on the removal of PO_4 (a) and NH_4 (b) from Solution (pH = 8.5; 100 rpm; contact time 40 minutes)

3.4. Effect of contact time

Figures 7a and 7b show the removal of PO_4^{3-} and NH_4^+ ions nutrients at pH 8.5 using 80 g/L adsorbent at different contact times, with the percentage of removal increasing with contact time, especially in the first 30 minutes. Figures 7a and 7b show that the modified zeolite affected the removed PO_4^{3-} and NH_4^+ ions. The results show that Zeo-Mg(1) modified zeolites removed more PO_4^{3-} and NH_4^+ ions than Zeo-Mg(2) modified zeolites and natural zeolites. According to Figure 7, the removal of PO_4^{3-} and NH_4^+ ions by the modified zeolite of Zeo-Mg (1) was 92.61% and 39.91%, respectively. This indicated that the activation method using Mg^{2+} ions at 80 °C was very effective in the ion exchange of K^+, Ca^{2+}, Fe^+ and Na^+ ions from the zeolite, which replaced their positions with Mg^{2+} ions as an adsorbing site. This resulted in fast diffusion and the rapid release of Mg^{2+} ions from the zeolite [48]. Furthermore, magnesium released from the zeolite reacts with PO_4^{3-} and NH_4^+ ions to form struvite. It can be seen in Figure 7 that the removal of PO_4^{3-} and NH_4^+ ions by natural zeolite quickly reached equilibrium within 20 and 40 minutes, respectively. There was a slight increase in the removal of PO_4^{3-} ions, which was mainly due to the slow ion exchange of Mg^{2+} ions from the natural zeolite. In other words, without any modification, natural zeolite is not suitable for struvite formation. Figure 7 shows that the equilibrium times across the three types of zeolites are not different, indicating that the amount of Mg ions in the zeolite did not significantly affect the equilibrium times. Similarly, Liu *et al*. [49] reported that a higher ratio of Mg/PO_4 did not significantly increase the amount of struvite formed from the reaction.

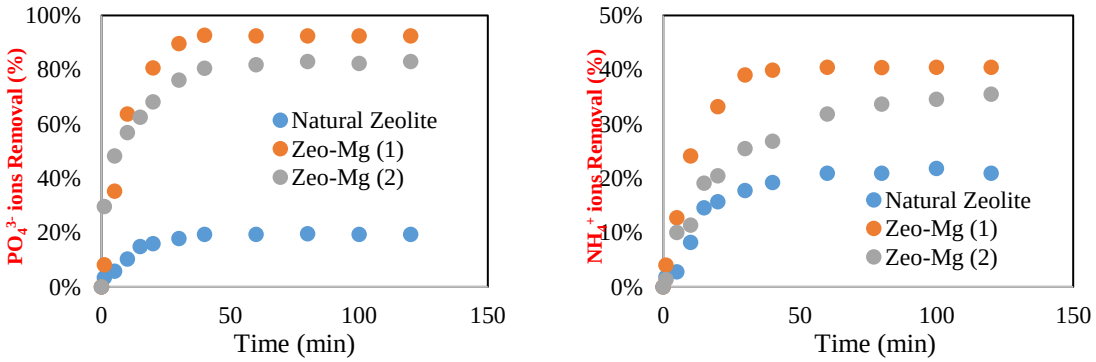

Figure 7: The effect of contact time on PO_4^{3-} (a) and NH_4^+ (b) removal at different modified zeolite (pH = 8.5; adsorbent dosage 80 g/L).

3.5. Kinetic Study of Modified Zeolite on the Removal of PO_4 and NH_4

The experimental data were used to estimate the kinetic mechanism by applying pseudo-first-order and pseudo-second-order kinetic models as presented in the following Equations 4 and 5, respectively [50]:

$$\log(q_e - q_t) = \log q_e - \frac{k_f}{2.303} t \quad (4)$$

$$\frac{t}{q_t} = \frac{1}{q_e} t + \frac{1}{k_s q_e^2} \quad (5)$$

Where q_t (mg/g) is the amount of adsorbate adsorbed at time t, q_e (mg/g) is the adsorption capacity at equilibrium, k_f (min.), and k_s (g/mg.min.) is the pseudo-first-order and pseudo-second-order rate constants, respectively. Pseudo-first-order and pseudo-second-order kinetic model parameters and values of linear regression coefficients are obtained from the respective fitted plots (Figure 8), which are tabulated in Tables 2 and 3. The experimental kinetic data were plotted as *log* $(q_e - q_t)$ against time (t), which generates a straight line with different slopes, as shown in Figures 8a and 8c, respectively. Further, the struvite crystallization is well exemplified by the pseudo-first-order kinetic model with a high correlation coefficient (R^2) above 0.977 for the removal of PO_4^{3-} and NH_4^+ ions using natural zeolites and modified zeolites. On the other hand, the pseudo-second-order kinetic model predicted by plotting t/q_e versus t showed that the experimental research data did not fit in a straight line (Figures 8b and 8c). The calculated (qe) values for the Pseudo-first order model for natural and modified zeolites were almost equivalent to the experimental (qe) values. For the removal of PO_4^{3-} ions (Table 2), the estimated rate constants were 0.0834, 0.1140, and 0.0827/min for natural zeolite, Zeo-Mg(1) and Zeo-Mg(2), respectively. Meanwhile, the estimated rate constants of NH_4^+ ions removal (Table 3) were 0.0617, 0.1069, and 0.0389 minutes for natural zeolite, Zeo-Mg(1) and Zeo-Mg(2), respectively. The pseudo-first-order model indicates that the struvite crystallization on natural and modified zeolite may be controlled by a physical adsorption process [51]. It is assumed that PO_4^{3-} and NH_4^+ ions are adsorbed onto the surface during the formation of crystal nuclei, thus preventing them from growing beyond the critical size.

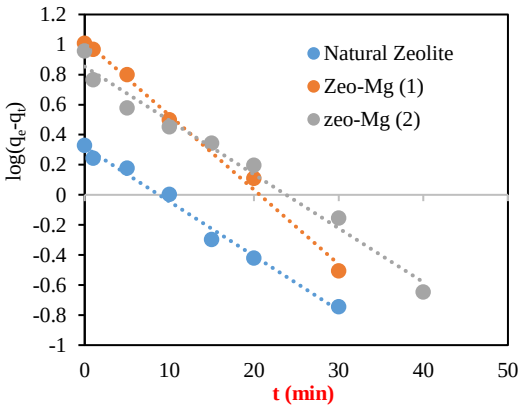

(a)

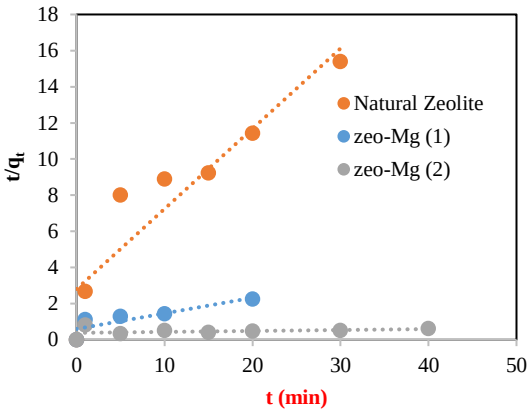

(b)

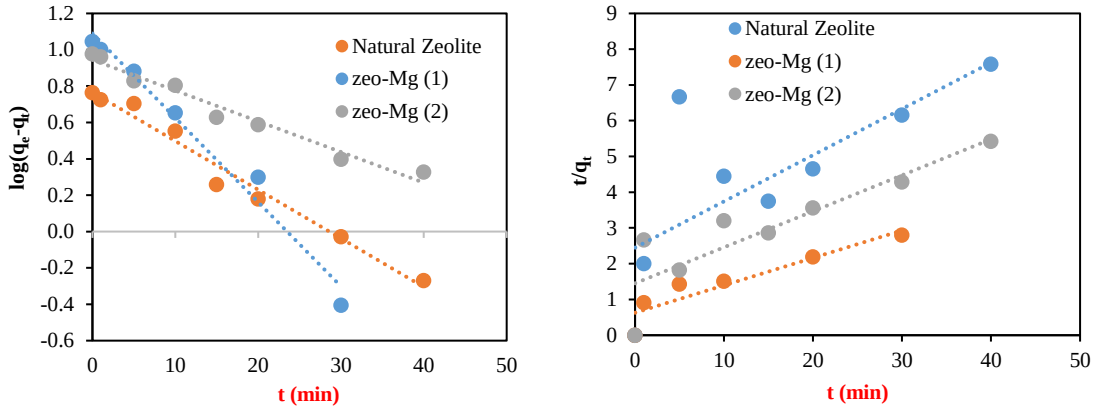

(c) (d)

Figure 8: Pseudo-first order and pseudo-second order for removal of PO_4^{3-} ions (a) (b) and NH_4^+ ions (c) (d) using natural and modified zeolites

Table 2: Kinetic parameters for removal of PO_4^{3-} and NH_4^+ ions for various kinetic models using natural and modified zeolites

Sample	Orde 1				Orde 2			
	k (/min)	q_e (mg/g) (experiment)	q_e (mg/g) (Calculation)	R^2	k (g/mg.min)	q_e (mg/g) (experiment)	q_e (mg/g) (Calculation)	R^2
Removal of PO_4^{3-} ions								
Natural Zeolite	0.0834	2.130	2.077	0.988	0.7852	2.130	2.25	0.873
Zeo-Mg(1)	0.1140	10.162	10.571	0.995	0.0162	10.162	11.59	0.761
Zeo-Mg(2)	0.0827	9.075	7.1351	0.979	0.0318	9.075	192.31	0.101
Removal of NH_4^+ ions								
Natural Zeolite	0.0617	5.813	5.830	0.977	0.0068	5.813	7.730	0.541
Zeo-Mg(1)	0.1069	11.119	12.283	0.977	0.0094	11.119	13.040	0.784
Zeo-Mg(2)	0.0389	9.500	8.8085	0.968	0.0070	9.500	9.920	0.865

Further data analysis identified the mechanisms involved in the adsorption system. The most common technique to identify the adsorption mechanism is the intra-particle diffusion model (Weber and J. C. Morris, 1963) as described in Equation 6 [52,53].

$$q_t = k_{id} t^{0.5} + C \quad (6)$$

Where k_{id} (mg/g.min$^{0.5}$) is the rate constant of intra-particle diffusion, $t^{0.5}$ is the half-life time in minutes, and C (mg/g) is a constant associated with the boundary layer thickness. The rate constant of k_{id} was determined from the slope of the straight line obtained by fitting the plot of q_t against $t^{0.5}$ as described in Equation 6 for the experimental data in Figure 9.

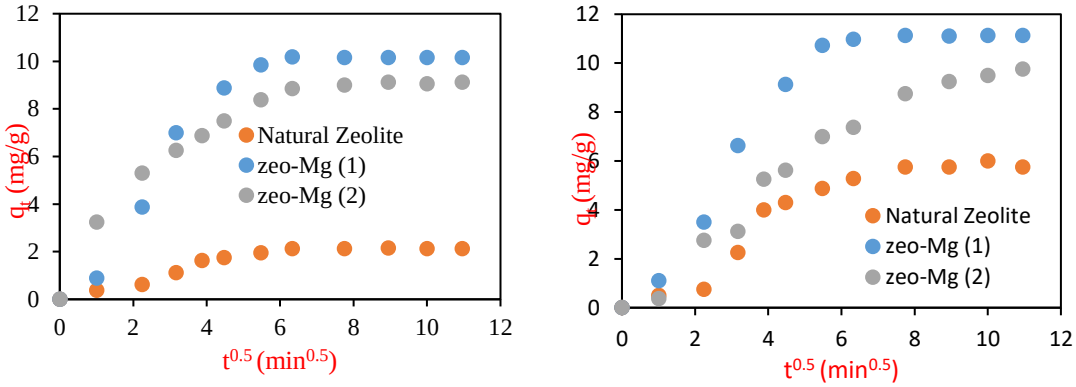

Figure 9: Intraparticle diffusion for removal of PO_4^{3-} and NH_4^+ ions

Figure 9 depicts plots with a straight line indicating the simultaneous occurrence of film diffusion and intra-particle diffusion, and that film diffusion may control struvite adsorption and crystallization on natural and modified zeolites at an earlier stage [54]. Essentially, there was a mass transfer of PO_4^{3-} and NH_4^+ ions from the bulk solution and Mg^{2+} ions released from the zeolite, and they react to form struvite and adsorb into the zeolite's surface via the boundary layer, then diffuse into the zeolite's interior.

Table 3: Intra-particle diffusion parameters

Sample	Kid	C	R2
	Removal of PO_4		
Natural Zeolite	0.3908	0.0753	0.9882
Zeo-Mg(1)	2.0433	0.5827	0.9946
Zeo-Mg(2)	1.1169	2.4941	0.9794
	Removal of NH_4		
Natural Zeolite	1.1295	1.0275	0.9512
Zeo-Mg(1)	2.2172	1.0342	0.9870
Zeo-Mg(2)	1.4217	0.9428	0.9726

The results of plotting the data in Figure 9 can be seen in Table 3. It was found that the zeolite modification could increase the K_{id} and C constants for PO_4^{3-} and NH_4^+ ions removal. A modification of Zeo-Mg(1) resulted in a higher diffusion rate constant (K_{id}) than Zeo-Mg(2) for both PO_4^{3-} and NH_4^+ ions removal. Further investigation revealed that the highest constant C for PO_4^{3-} ion removal occurred on Zeo-Mg(2), whereas NH_4^+ ion adsorption occurred on Zeo-Mg(1). A high value of C indicates that the rate of the adsorption mechanism is influenced by the limiting boundary layer, suggesting a higher contribution of the surface sorption in the rate-limiting stage [55,57].

4. Conclusions

The simultaneous removal of PO_4^{3-} and NH_4^+ ions from the solution was investigated using natural and modified zeolite as the adsorbent materials in struvite crystallization. The results showed that the removal of PO_4^{3-} and NH_4^+ ions from the solution mainly depends on modified zeolite and the crystallization of struvite. The highest removal of PO_4^{3-} and NH_4^+ ions was 93.32% and 42.45%, respectively, achieved at pH 8.5 with a dosage of modified zeolite Zeo-Mg (l) by 80 g/L. The pseudo-first-order kinetic model agreed well with the data for the

adsorption of PO_4^{3-} and NH_4^+ ions, and the SEM-EDS and FT-IR of natural and modified zeolite confirmed the presence of struvite.

References

[1] H. Wang, X. Wang, and J. Zhao, "Application of MgO-Modified palygorskite for Nutrient Recovery from Swine Wastewater: Effect of pH, Ions, and Organic Acids," *Environ. Sci. Pollut. Res.*, vol. 26, no. 19, pp. 19729-19737, 2019.

[2] E. Ariyanto, T. K. Sen, and H. M. Ang, "The influence of various physico-chemical process parameters on kinetics and growth mechanism of struvite crystallisation," *Adv. Powder Technol.*, vol. 25, no. 2, pp. 682-694, 2014.

[3] A. Escudero, F. Blanco, A. Lacalle, and M. Pinto, "Struvite precipitation for ammonium removal from anaerobically treated effluents," *J. Environ. Chem. Eng.*, vol. 3, no. 1, pp. 413-419, 2015.

[4] S. A. Parsons and J. D. Doyle, "Struvite formation, control and recovery," *Water Res.*, vol. 36, no. 16, pp. 3925-3940, 2002.

[5] Y. Wang, J. Mou, X. Liu, and J. Chang, "Phosphorus recovery from wastewater by struvite in response to initial nutrients concentration and nitrogen/phosphorus molar ratio," *Sci. Total Environ.*, vol. 789, no. 10, pp. 1-10 2021.

[6] M. Quintana, E. Sánchez, M. F. Colmenarejo, J. Barrera, G. García, and R. Borja, "Kinetics of phosphorus removal and struvite formation by the utilization of by-product of magnesium oxide production," *Chem. Eng. J.*, vol. 111, no. 1, pp. 45-52, 2005.

[7] E. Ariyanto, H. M. Ang, and T. K. Sen, "Impact of various physico-chemical parameters on spontaneous nucleation of struvite (MgNH4PO4.6H2O) formation in a wastewater treatment plant: kinetic and nucleation mechanism," *Desalin. Water Treat.*, vol. 52, no. 34-36, pp. 6620-6631, 2014.

[8] D. Kim, K. J. Min, K. Lee, M. S. Yu, and K. Y. Park, "Effects of pH, molar ratios and pre-treatment on phosphorus recovery through struvite crystallization from effluent of anaerobically digested swine wastewater," *Environ. Eng. Res.*, vol. 22, no. 1, pp. 12-18, 2017.

[9] N. O. Nelson, R. L. Mikkelsen, and D. L. Hesterberg, "Struvite precipitation in anaerobic swine lagoon liquid: Effect of pH and Mg:P ratio and determination of rate constant," *Bioresour. Technol.*, vol. 89, no. 3, pp. 229-236, 2003.

[10] F. Mijangos, M. Kamel, G. Lesmes, and D. N. Muraviev, "Synthesis of struvite by ion exchange isothermal supersaturation technique," *React. Funct. Polym.*, vol. 60, no. 1-3, pp. 151-161, 2004.

[11] H. Huang, D. Xiao, R. Pang, C. Han, and L. Ding, "Simultaneous Removal of Nutrients from Simulated Swine Wastewater by Adsorption of Modified Zeolite Combined with Struvite Crystallization," *Chem. Eng. J.*, vol. 256, no. 4, pp. 431-438, 2014.

[12] J. Guo, C. Yang, and G. Zeng, "Treatment of swine wastewater using chemically modified zeolite and bioflocculant from activated sludge," *Bioresour. Technol.*, vol. 143, no. 9, pp. 289-297, 2013.

[13] S. Montalvo, L. Guerrero, R. Borja, E. Sánchez, Z. Milán, I. Cortés, and M. A. Rubia, "Application of natural zeolites in anaerobic digestion processes: A review," *Appl. Clay Sci.*, vol. 58, no. 4, pp. 125-133, 2012.

[14] H. N. Yeritsyan, S. K. Nickoghosyan, A. A. Sahakyan, V. V. Harutunyan, E. A. Hakhverdyan, and N. E. Grigoryan, *Comparative analyses of physical properties of natural zeolites from Armenia and USA*, vol. 174, no. SUPPL. PART A. 2008.

[15] S. M. Al-Jubouri, S. I. Al-Batty, S. Senthilnathan, N. Sihanonth, L. Sanglura, H. Shan, and S. M. Holmes, "Utilizing faujasite-type zeolites prepared from waste aluminum foil for competitive ion-exchange to remove heavy metals from simulated wastewater," *Desalin. Water Treat.*, vol. 231, no. 8, pp. 166-181, 2021.

[16] A. Alshameri, C. Yan, Y. Al-Ani, A. S. Dawood, A. Ibrahim, C. Zhou, and H. Wang, "An investigation into the adsorption removal of ammonium by salt activated Chinese (Hulaodu) natural zeolite: Kinetics, isotherms, and thermodynamics," *J. Taiwan Inst. Chem. Eng.*, vol. 45, no. 2, pp. 554-564, 2014.

[17] L. Lin, Z. Lei, L. Wang, X. Liu, Y. Zhang, C. Wan, D. J. Lee, and J. H. Tay, "Adsorption mechanisms of high-levels of ammonium onto natural and NaCl-modified zeolites," *Sep. Purif. Technol.*, vol. 103, no. 1, pp. 15-20, 2013.

[18] Y. Watanabe, H. Yamada, J. Tanaka, and Y. Moriyoshi, "Hydrothermal modification of natural zeolites to improve uptake of ammonium ions," *J. Chem. Technol. Biotechnol.*, vol. 80, no. 4, pp.

376-380, 2005.
[19] J. Shi, Z. Yang, H. Dai, X. Lu, L. Peng, X. Tan, L. Shi, and R. Fahim, "Preparation and application of modified zeolites as adsorbents in wastewater treatment," *Water Sci. Technol.*, vol. 2017, no. 3, pp. 621-635, 2017.
[20] Z. Liang and J. Ni, "Improving the ammonium ion uptake onto natural zeolite by using an integrated modification process," *J. Hazard. Mater.*, vol. 166, no. 1, pp. 52-60, 2009.
[21] L. Lei, X. Li, and X. Zhang, "Ammonium removal from aqueous solutions using microwave-treated natural Chinese zeolite," *Sep. Purif. Technol.*, vol. 58, no. 3, pp. 359-366, 2008.
[22] O. Lahav, Y. Schwartz, P. Nativ, and Y. Gendel, "Sustainable removal of ammonia from anaerobic-lagoon swine waste effluents using an electrochemically-regenerated ion exchange process," *Chem. Eng. J.*, vol. 218, pp. 214-222, 2013.
[23] N. Karapinar, "Application of natural zeolite for phosphorus and ammonium removal from aqueous solutions," *J. Hazard. Mater.*, vol. 170, no. 2-3, pp. 1186-1191, 2009.
[24] E. Marañón, M. Ulmanu, Y. Fernández, I. Anger, and L. Castrillón, "Removal of ammonium from aqueous solutions with volcanic tuff," *J. Hazard. Mater.*, vol. 137, no. 3, pp. 1402-1409, 2006.
[25] K. Saltali, A. Sari, and M. Aydin, "Removal of ammonium ion from aqueous solution by natural Turkish (Yıldızeli) zeolite for environmental quality," *J. Hazard. Mater.*, vol. 141, no. 1, pp. 258-263, 2007.
[26] Q. Du, S. Liu, Z. Cao, and Y. Wang, "Ammonia removal from aqueous solution using natural Chinese clinoptilolite," *Sep. Purif. Technol.*, vol. 44, no. 3, pp. 229-234, 2005.
[27] A. Thornton, P. Pearce, and S. A. Parsons, "Ammonium removal from solution using ion exchange on to MesoLite, an equilibrium study," *J. Hazard. Mater.*, vol. 147, no. 3, pp. 883-889, 2007.
[28] H. Huang, X. Xiao, B. Yan, and L. Yang, "Ammonium removal from aqueous solutions by using natural Chinese (Chende) zeolite as adsorbent," *J. Hazard. Mater.*, vol. 175, no. 1-3, pp. 247-252, 2010.
[29] E. Saputra, M. A. Budihardjo, S. Bahri, and J. A. Pinem, "Cobalt-exchanged natural zeolite catalysts for catalytic oxidation of phenolic contaminants in aqueous solutions," *J. Water Process Eng.*, vol. 12, pp. 47-51, 2016.
[30] S. M. Al-Jubouri, S. I. Al-Batty, R. Ramsden, J. Tay, and S. M. Holmes, "Elucidation of the removal of trivalent and divalent heavy metal ions from aqueous solutions using hybrid-porous composite ion-exchangers by nonlinear regression," *Desalin. Water Treat.*, vol. 236, pp. 171-181, 2021.
[31] M. Sadrara, M. Khanmohammadi Khorrami, J. Towfighi Darian, and A. Bagheri Garmarudi, "Rapid determination and classification of zeolites based on Si/Al ratio using FTIR spectroscopy and chemometrics," *Infrared Phys. Technol.*, vol. 116, no. May, p. 103797, 2021.
[32] H. J. Choi, S. W. Yu, and K. H. Kim, "Efficient use of Mg-modified zeolite in the treatment of aqueous solution contaminated with heavy metal toxic ions," *J. Taiwan Inst. Chem. Eng.*, vol. 63, pp. 482-489, 2016.
[33] Y. Yu, J. G. Shapter, R. Popelka-Filcoff, J. W. Bennett, and A. V. Ellis, "Copper removal using bio-inspired polydopamine coated natural zeolites," *J. Hazard. Mater.*, vol. 273, pp. 174-182, 2014.
[34] M. Ostrooumov, P. Cappelletti, and R. de'Gennaro, "Mineralogical study of zeolite from New Mexican deposits (Cuitzeo area, Michoacan, Mexico)," *Appl. Clay Sci.*, vol. 55, pp. 27-35, 2012.
[35] J. Coates, "Interpretation of Infrared Spectra, A Practical Approach," *Encycl. Anal. Chem.*, pp. 1-23, 2006.
[36] Lalhmunsiama, D. Tiwari, and S. M. Lee, "Surface-functionalized activated sericite for the simultaneous removal of cadmium and phenol from aqueous solutions: Mechanistic insights," *Chem. Eng. J.*, vol. 283, pp. 1414-1423, 2016.
[37] D. Li, J. Zhou, Y. Wang, Y. Tian, L. Wei, Z. Zhang, Y. Qiao, and J. Lia, "Effects of activation temperature on densities and volumetric CO_2 adsorption performance of alkali-activated carbons," *Fuel*, vol. 238, no. June 2018, pp. 232-239, 2019.
[38] Y. Zhang, Y. Cong, J. Zhang, X. Li, Y. Li, Z. Dong, G. Yuan, J. Zhang, and Z. Cui, "Effects of activation temperatures on the surface structures and supercapacitive performances of porous carbon fibers," *Surf. Coatings Technol.*, vol. 349, no. June, pp. 384-391, 2018.
[39] M. Prabhu and S. Mutnuri, "Cow urine as a potential source for struvite production," *Int. J. Recycl. Org. Waste Agric.*, vol. 3, no. 1, pp. 1-12, 2014.

[40] J. Slavek and W. F. Pickering, "The Effect of pH On The Retention of Cu, Pb, Cd, and Zn By Clay - Fulvic Acid Mixtures," *Water. Air. Soil Pollut.*, vol. 8, pp. 209-221, 1981.

[41] J. Chen, H. Kong, D. Wu, Z. Hu, Z. Wang, and Y. Wang, "Removal of phosphate from aqueous solution by zeolite synthesized from fly ash," *J. Colloid Interface Sci.*, vol. 300, no. 2, pp. 491-497, 2006.

[42] N. Hamdi and E. Srasra, "Removal of phosphate ions from aqueous solution using Tunisian clays minerals and synthetic zeolite," *J. Environ. Sci.*, vol. 24, no. 4, pp. 617-623, 2012.

[43] Z. Lu, K. Zhang, F. Liu, X. Gao, Z. Zhai, J. Li, and L. Du,, "Simultaneous recovery of ammonium and phosphate from aqueous solutions using Mg/Fe modified NaY zeolite: Integration between adsorption and struvite precipitation," *Sep. Purif. Technol.*, vol. 299, no. July, p. 121713, 2022.

[44] P. V. Haseena, K. S. Padmavathy, P. R. Krishnan, and G. Madhu, "Adsorption of Ammonium Nitrogen from Aqueous Systems Using Chitosan-Bentonite Film Composite," *Procedia Technol.*, vol. 24, pp. 733-740, 2016.

[45] D. Hsu, C. Lu, T. Pang, Y. Wang, and G. Wang, "Adsorption of ammonium nitrogen from aqueous solution on chemically activated biochar prepared from sorghum distillers grain," *Appl. Sci.*, vol. 9, no. 23, pp. 1-16, 2019.

[46] I. Stratful, M. D. Scrimshaw, and J. N. Lester, "Conditions influencing the precipitation of magnesium ammonium phosphate," *Water Res.*, vol. 35, no. 17, pp. 4191-4199, 2001.

[47] P. Xia, X. Wang, X. Wang, J. Zhang, H. Wang, J. Song, R. Ma, J. Wang, and J. Zhao, "Synthesis and characterization of MgO modified diatomite for phosphorus recovery in eutrophic water," *J. Chem. Eng. Data*, vol. 62, no. 1, pp. 226-235, 2017.

[48] D. Karadag, Y. Koc, M. Turan, and B. Armagan, "Removal of ammonium ion from aqueous solution using natural Turkish clinoptilolite," *J. Hazard. Mater.*, vol. 136, no. 3, pp. 604-609, 2006.

[49] X. Liu, G. Wen, Z. Hu, and J. Wang, "Coupling effects of pH and Mg/P ratio on P recovery from anaerobic digester supernatant by struvite formation," *J. Clean. Prod.*, vol. 198, no. 10, pp. 633-641, 2018.

[50] S. Dawood, T. K. Sen, and C. Phan, "Synthesis and characterisation of novel-activated carbon from waste biomass pine cone and its application in the removal of congo red dye from aqueous solution by adsorption," *Water. Air. Soil Pollut.*, vol. 225, no. 1, pp. 1-16, 2014.

[51] M. Ghasemi, N. Ghasemi, G. Zahedi, S. R. W. Alwi, M. Goodarzi, and H. Javadian, "Kinetic and equilibrium study of Ni(II) sorption from aqueous solutions onto Peganum harmala-L," *Int. J. Environ. Sci. Technol.*, vol. 11, no. 7, pp. 1835-1844, 2014.

[52] S. M. Al-Jubouri, H. A. Al-Jendeel, S. A. Rashid, and S. Al-Batty, "Antibiotics adsorption from contaminated water by composites of ZSM-5 zeolite nanocrystals coated carbon," *J. Water Process Eng.*, vol. 47, no. January, p. 102745, 2022.

[53] N. Magesh, A. A. Renita, R. Siva, N. Harirajan, and A. Santhosh, "Adsorption behavior of fluoroquinolone(ciprofloxacin) using zinc oxide impregnated activated carbon prepared from jack fruit peel: Kinetics and isotherm studies," *Chemosphere*, vol. 290, no. December 2021, p. 133227, 2022.

[54] S. Dawood, T. K. Sen, and C. Phan, "Adsorption removal of Methylene Blue (MB) dye from aqueous solution by bio-char prepared from Eucalyptus sheathiana bark: kinetic, equilibrium, mechanism, thermodynamic and process design," *Desalin. Water Treat.*, vol. 57, no. 59, pp. 28964-28980, 2016.

[55] S. Dawood, T. K. Sen, and C. Phan, "Synthesis and characterization of slow pyrolysis pine cone bio-char in the removal of organic and inorganic pollutants from aqueous solution by adsorption: Kinetic, equilibrium, mechanism and thermodynamic," *Bioresour. Technol.*, vol. 246, no. 12, pp. 76-81, 2017.

[56] Yasser Yousef Muhi-Alden, Khulood A. Saleh, "Removing of Methylene Blue Dye from its Aqueous Solutions Using Polyacrylonitrile/Iron Oxide/Graphene Oxide", *Iraqi Journal of Science*, vol. 63, no. 6, pp. 2320-2330, 2022

[57] Israa T. Ali1 , Namir I. A. Haddad1 *, Ekhlas A. Hussein, "Assessment of Monocyte Chemo-Attractant Protein-1 (MCP-1) and Other Biochemical Parameters in Iraqi Pregnant Women", *Iraqi Journal of Science*, vol. 63, no. 10, pp. 4152-4162, 2022.